Left ventricular hypertrophy index based on a combination of frontal and transverse planes in the ECG and VCG: Diagnostic utility of cardiac vectors

Maria Paula Bonomini[14], Fernando Juan Ingallina[2], Valeria Barone[2], Ricardo Antonucci[2], Max Valentinuzzi[1], Pedro David Arini[1,3]

[1] Intituto de Ingeniería Biomédica (IIBM), Facultad de Ingeniería, UBA, Buenos Aires, Argentina,
[2] Instituto de Investigaciones Médicas "Dr. Alfredo Lanari", UBA, Buenos Aires, Argentina,
[3] Instituto Argentino de Matemáticas "Alberto P. Calderón", CONICET, Buenos Aires, Argentina

E-mail: paulabonomini@gmail.com

Abstract. The changes that left ventricular hypertrophy (LVH) induces in depolarization and repolarization vectors are well known. We analyzed the performance of the electrocardiographic and vectorcardiographic transverse planes (TP in the ECG and XZ in the VCG) and frontal planes (FP in the ECG and XY in the VCG) to discriminate LVH patients from control subjects. In an age-balanced set of 58 patients, the directions and amplitudes of QRS-complexes and T-wave vectors were studied. The repolarization vector significantly decreased in modulus from controls to LVH in the transverse plane (TP: 0.45±0.17mV vs. 0.24±0.13mV, $p<0.0005$; XZ: 0.43±0.16mV vs. 0.26±0.11mV, $p<0.005$) while the depolarization vector significantly changed in angle in the electrocardiographic frontal plane (Controls vs. LVH, FP: 48.24±33.66° vs. -46.84±35.44°, $p<0.005$, XY: 20.28±35.20° vs. 19.35±12.31°, NS). Several LVH indexes were proposed combining such information in both ECG and VCG spaces. A subset of all those indexes with AUC values greater than 0.7 was further studied. This subset comprised four indexes, with three of them belonging to the ECG space. Two out of the four indexes presented the best ROC curves (AUC values: 0.78 and 0.75, respectively). One index belonged to the ECG space and the other one to the VCG space. Both indexes showed a sensitivity of 86% and a specificity of 70%. In conclusion, the proposed indexes can favorably complement LVH diagnosis

1. Introduction

LVH indexes based only on the electrocardiogram are known to present low sensitivity and high specificity. Although it is well known that repolarization is also modified with LVH [1, 2, 3], attempts to include this information in electrocardiographic indexes [4] fell into disuse, focusing all efforts on different features of the depolarization phase [5, 6].

There has also been a longstanding disagreement as to whether the ECG or VCG spaces appears as more informative, with reports showing the VCG as better [7, 8], similar [6] or poorer [9] than the ECG for LVH diagnosis.

[4] Present address: Instituto de Ingeniería Biomédica, Facultad de Ingeniería, Universidad de Buenos Aires (UBA), Paseo Colón 850, Argentina.

Herein, we have combined depolarization and repolarization information in the transverse and frontal planes to construct a set of LVH indexes and compared their diagnosis performance in the ECG and VCG spaces. Therefore, we compared the performance of these indexes in two sets of equivalent planes: (1): the electrocardiographic frontal plane (FP) versus the vectorcardiographic frontal plane (XYP), (2): the electrocardiographic transverse plane (TP) versus the vectorcardiographic transverse plane (XZP).

2. Materials and Methods

2.1. Population

A total of 58 subjects without intraventricular conduction disturbances were retrospectively studied. Two groups were balanced for age characteristics: the LVH group (31 subjects, mean age 68.5±12.3 years old) and the control group (27 subjects, mean age 60.6±13.2 years old). The hypertrophy group included patients with left ventricular mass indexes greater than 125 g/m^2 in males and greater than 110 g/m^2 in females, as calculated by Devereux's formula from echocardiography on M-mode [10]. These patients lacked a coronary artery disease history. Healthy subjects, without clinical or echocardiographic evidence of cardiovascular disease, comprised the Control group. Besides echocardiographic data, 5-minute 12-lead ECG recordings were taken from all the subjects. Patients were recruited in the medical institution *"Instituto de Investigaciones Medicas, Dr. Alfredo Lanari" of the University of Buenos Aires* and in all cases informed consent was signed.

2.2. ECG Preprocessing

Signal preprocessing was applied to the 12 standard ECG leads, implementing QRS-detection and normal beat selection according to the method given in reference [11]. The QRS-complexes and T-waves were located and delineated using the wavelet transform based method described in [12] and baseline wandering attenuation was treated by cubic spline. Noisy beats were rejected when differences in mean isoelectric level with respect to adjacent beats were larger than 300 μV.

VCG was synthesized by means of the Kors Matrix [13]. The XZP was obtained from the VCG signals while the TP was derived from the standard ECG signals. More specifically, the precordial leads V_6 and $V_{1\text{-}2}$ were used, being the latter an average between leads V_1 and V_2.

2.3. Cardiac vectors

Cardiac vectors were measured in all planes following the same methodology as the one used here for the TP. Segmentation of the QRS-complex and T-wave was accomplished for each i_{th} beat using a single lead criterion, where the respective QRS and T onsets were taken at the earliest reliable QRS and T, either for V_6 or for $V_{1\text{-}2}$. The offsets, in a symmetric way, were accepted respectively as the latest reliable QRS-complex and T-wave offsets for the same leads, as in the previous case. On these segmented waves, the QRS-loop and the T-wave loop for each i_{th} beat were constructed and both cardiac vectors computed for the loop samples $\mathrm{n} \in W_i^{\mathrm{QRS}}$ and $\mathrm{n} \in W_i^{\mathrm{T}}$, representing the QRS-complex and T-wave windows respectively. The samples $n_{\max}^{\mathrm{QRS}}(i)$ and $n_{\max}^{\mathrm{T}}(i)$ at which the respective QRS-complex and T-wave cardiac vectors resulted maximum were also computed. Thereafter, the angle and modulus of the QRS-complex main cardiac vector for the i_{th} beat, $R_H^{\alpha}(i)$ and $R_H^{m}(i)$ respectively, were defined as,

$$R_H^{\alpha}(i) = \operatorname{atan}\left(\frac{V_{1\text{-}2}(n_{\max}^{\mathrm{QRS}}(i))}{V_6(n_{\max}^{\mathrm{QRS}}(i))}\right) \tag{1}$$

$$R_H^{m}(i) = \sqrt{V_6(n_{\max}^{\mathrm{QRS}}(i))^2 + V_{1\text{-}2}(n_{\max}^{\mathrm{QRS}}(i))^2} \tag{2}$$

where,

$$n_{\max}^{\mathrm{QRS}}(i) = \arg\max_{n} \left[\sqrt{V_6(n)^2 + V_{1\text{-}2}(n)^2} \right] \tag{3}$$

where n $\in W_i^{\mathrm{QRS}}$

Notice that subscript H instead of T is used for denoting the transverse plane. This is so to avoid confusions with repolarization parameters.

Analogously, the angle and modulus of the T-wave maximum cardiac vector for the i_{th} beat, $T_H^{\alpha}(i)$ and $T_H^{m}(i)$ respectively, were defined as in (1)-(3) for n $\in W_i^{\mathrm{T}}$.

The angle and modulus of the main depolarization vectors for the i_{th} beat, $R_F^{\alpha}(i)$, $R_{XZ}^{\alpha}(i)$, $R_{XY}^{\alpha}(i)$ and $R_F^{m}(i)$, $R_{XZ}^{m}(i)$, $R_{XY}^{m}(i)$ respectively, as well as the angle and modulus of the T-wave maximum cardiac vectors for the i_{th} beat, $T_F^{\alpha}(i)$, $T_{XZ}^{\alpha}(i)$, $T_{XY}^{\alpha}(i)$ and $T_F^{m}(i)$, $T_{XZ}^{m}(i)$, $T_{XY}^{m}(i)$ were defined as in (1)-(3).

2.4. LVH indexes

LVH indexes consisted of relations between angle and modulus of the cardiac vectors combining phases (depolarization/repolarization) and planes (frontal/transverse in ECG; XYP/XZP in VCG). Afterwards, Receiver Operative Characteristic (ROC) curves were computed for every index, and a subset with all those indexes with the area under the curve (AUC) values greater than 0.70 was selected for further analysis.

2.5. Statistical Analyses

All data were expressed as Mean±SD. The D'Agostino-Pearson normality test was applied to quantify the discrepancy between the distribution of the indexes and an ideal Gaussian distribution. In order to determine the statistical power of each marker to discriminate health from hypertrophy, a non-parametric two-tailed Mann-Whitney test was applied between controls and LVH patients. When p- value was <0.05, differences were considered statistically significant.

3. Results

Figure 1 shows the dominant depolarization and repolarization vectors for the control and the hypertrophy groups for every plane in both ECG and VCG spaces. These vectors resulted from averaging the i_{th} beat-dominant vectors accross all patients within each group. The complete numerical values and statistical significance can be found in Table 1.

LVH indexes based on amplitude and angle relationships of the above calculated vectors and their corresponding ROC curves and areas were computed. Figure 2 shows the AUC values for every index under study in both the ECG and VCG space. Notice that four out of ten indexes produced AUC values greater than 0.70. The latter indexes were: T_H^{α}/T_H^{m}, R_H^{α}/T_H^{m}, R_F^{α}/T_H^{m} and R_H^{α}/T_F^{m}. Notice that three out of four indexes in this selected subset combined depolarization and repolarization information in both representations: the frontal and transverse planes and all the three of them belonged to the ECG space.

The ROC curves for the four pairs of LVH indexes with AUC values greater than 0.70 together with their ECG(VCG) counterparts are displayed in Figure 3. The optimal cut-off point in the ROC curves were computed as the point nearest to the top left-hand corner. This selection maximizes the sensitivity and specificity sum, when it is assumed that the 'cost' of a false negative result is the same as that of a false positive one [14]. Characterization of the cut-off points are also shown in the paired format (Sensitivity; Specificity).

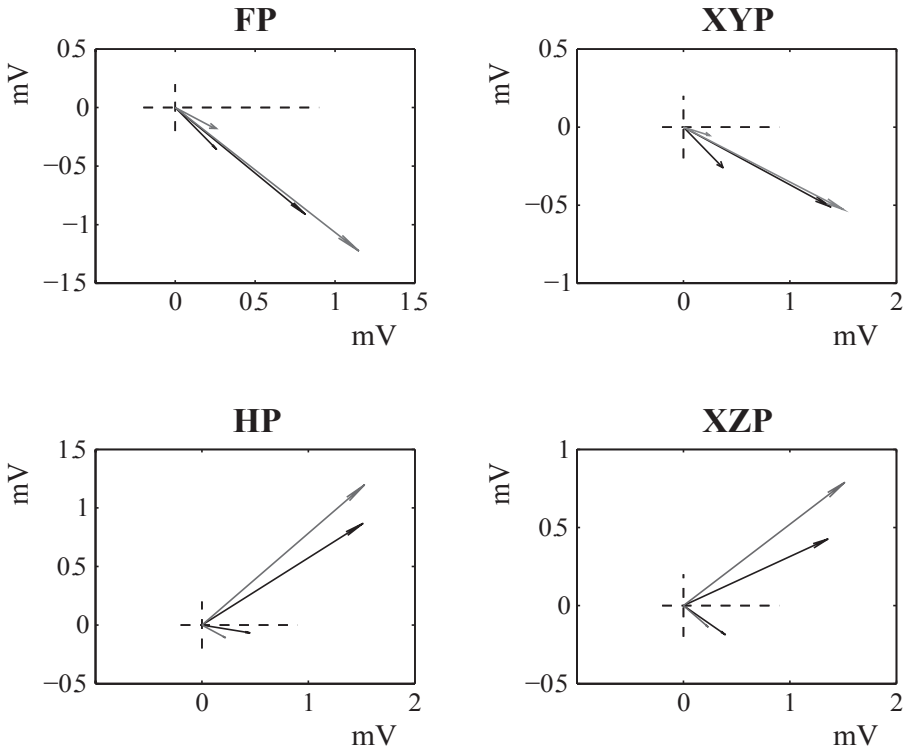

Figure 1. Mean depolarization and repolarization vectors for controls (solid lines) and LVH (grey line) groups.

Table 1. Mean±SD values for every parameter in control and LVH groups. * $p<0.05$, # $p<0.005$, & $p<0.0005$. 1: Frontal Plane (FP), 2: transverse plane (TP), 3: XY plane (XYP), 4: XZ plane (XZP)

	Controls				LVH			
	$R^{\alpha}[^{o}]$	R^{m}[mV]	$T^{\alpha}[^{o}]$	T^{m}[mV]	$R^{\alpha}[^{o}]$	R^{m}[mV]	$T^{\alpha}[^{o}]$	T^{m}[mV]
1	48.24±33.66$^{\#}$	1.22±0.44*	54.08±25.17*	0.44±0.20$^{\#}$	-46.84±35.44	1.68±0.79	35.78±42.20	0.30±0.12
2	-29.83±28.00	1.74±0.41	8.45±33.80	0.45±0.17$^{\&}$	-38.12±24.58	1.93±1.09	26.09±50.22	0.24±0.13
3	20.28±35.20	1.47±0.35	35.01±16.61	0.45±0.17$^{\&}$	19.35±12.31	1.59±0.74	12.20±62.00	0.25±0.10
4	-17.39±31.37	1.42±0.34	25.38±26.25*	0.43±0.16$^{\&}$	-27.49±35.18	1.70±0.82	30.85±57.56	0.26±0.11

4. Discussion

Four ECG-based LVH index combining features from the QRS-complex and the T-wave in both transverse and frontal planes were presented. Although it has been well described that LVH alters both depolarization and repolarization phases [15, 3], no utilization of the T-wave amplitude in LVH diagnosis has been reported in the clinical practice. ECG describes the electrophysiological remodelling induced by LVH, consisting of a ventricular conduction delay [16] and a prolongation of the action potential duration [17]. Thus, the final repolarization changes such as amplitude, axis and loop morphology result from the interplay with the depolarization modifications induced by LVH. These changes were classified into primary and secondary repolarization changes by Bacharova et al. [3] . This depolarization/repolarization interplay, makes it even harder to obtain clear ECG/VCG patterns when studied the cardiac

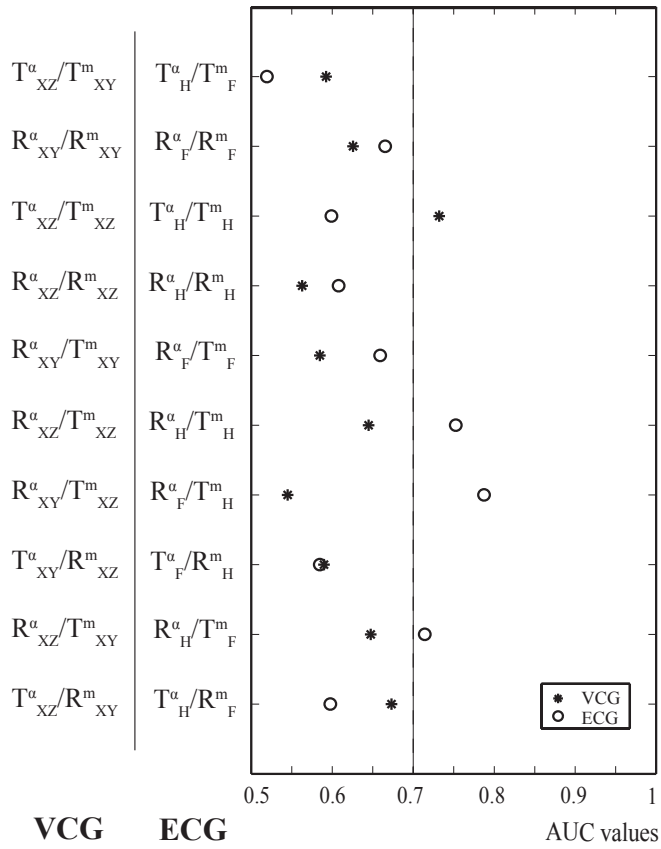

Figure 2. AUC values for all the LVH indexes proposed. AUC values for every index are plotted for the ECG (asterisks) and the VCG (circles) counterparts.

phases isolatedly. The main hypothesis applied herein was that cardiac vectors compensate for this particular fluctuations and show a more robust behavior to the LVH-induced changes when studied simultaneously.

On the other hand, the best performance of R^{α}_{F}/T^{m}_{H} is greatly supported by the literature. The Romhilt-Estes score includes the electrical axis in the frontal plane [18] and the amplitude of the T-wave has been a LVH marker in hypertrophic patients without ECG criteria for LVH [19]. Finally, even though angle and modulus of the vectors conforming the index were calculated from the depolarization and repolarization loops, which are mathematical constructions, the equivalent elements, namely, the left axis deviation in the frontal plane and the T-wave amplitude in the transverse plane (V_6 in this case) can be easily obtained in the clinical scenario, providing an efficient LVH index fully available with a 12-leads ECG record.

5. Conclusion

Most of the LVH indexes with a good performance to separate out LVH patients from controls belonged to the ECG space, vindicating the ECG for LVH diagnosis. The best electrocardiographic LVH index derived from this analysis, R^{α}_{F}/T^{m}_{H} combined depolarization and repolarization parameters suggesting that repolarization would greatly contribute to LVH diagnosis.

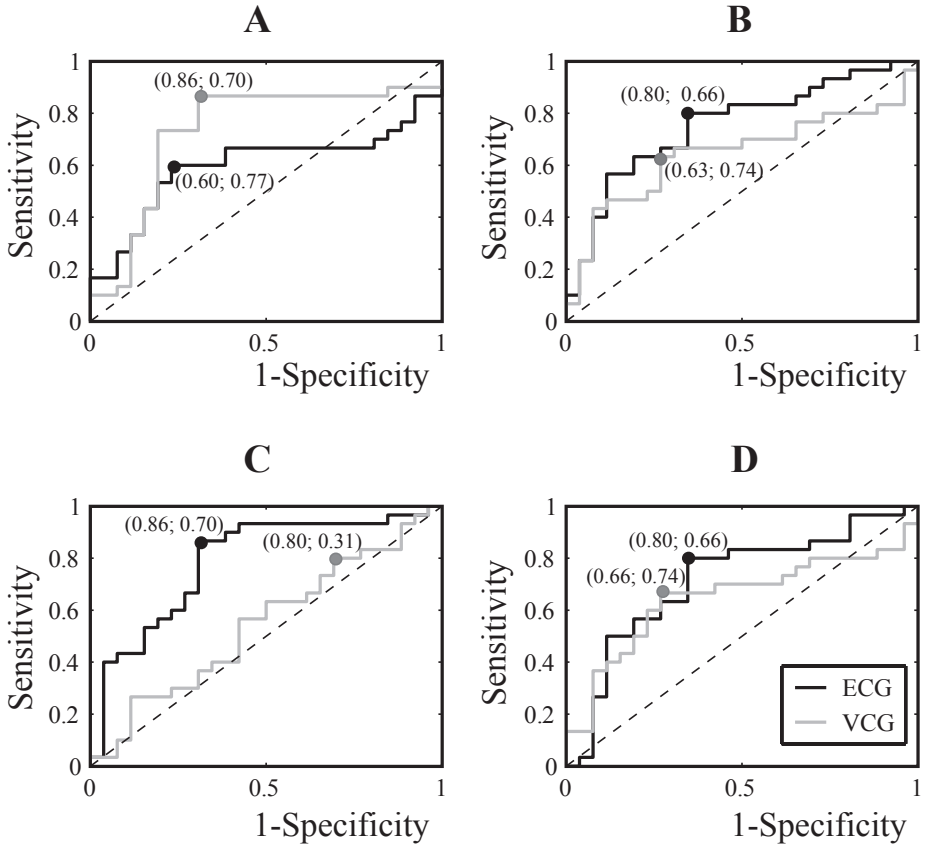

Figure 3. ROC curves for the subset of LVH indexes with AUC values greater than 0.7. A): $R^{\alpha}_{XZ}/T^{m}_{XZ}$, B): R^{α}_{H}/T^{m}_{H}, C): R^{α}_{F}/T^{m}_{H} and D): R^{α}_{H}/T^{m}_{F}. Every index is plotted with the ECG (black) and VCG (grey) counterparts.

Acknowledgements
This work was supported by the Consejo Nacional de Investigaciones Científicas y Técnicas, under Project PIP-538 and PICT 2008 #2108 Agencia Nacional de Promoción Científica y Tecnológica, Argentina.

6. References

[1] Bacharova L 2009 *Journal of Electrocardiology* **42** 388–91
[2] Bacharova L 2009 *Journal of Electrocardiology* **42** 593:96
[3] Bacharova L, Szathmary V and Mateasik A 2010 *J. of Electrocardiology* **43(6)** 624–33
[4] Casale P, Devereux R, Kligfield P, Eisenberg R, Miller D, Chaudhary B and Phillips M 1985 *J Am Coll Cardiol.* **6** 572–80
[5] Sokolow M and Lyon T 1949 *Am. Heart. J.* **37** 161–86
[6] Romhilt D, Greenfield J and Estes E 1968 *Circulation* **XXXVII** 15–19
[7] Bristow J, Porter G and H G 1961 *Am Heart J.* **62** 621
[8] Pérez Riera A, Uchida A, Filho C, Meneghini A, Ferreira C, Schapacknik E, Dubner S and Moffa P 2007 *Clin Cardiol.* **30(7)** 319–23
[9] Borun E, Chapman J and Massey F 1966 *Am. J. Cardiol.* **18** 656
[10] Devereux R B and Reichek N 1977 *Circulation* **55** 613–8
[11] Pan J and Tompkins W J 1985 *Biomedical Engineering, IEEE Transactions on* **BME-32** 230–236
[12] Mendieta J 2012 *Algoritmo para el delineado de senales electrocardiograficas en un modelo animal empleando*

tecnicas avanzadas de procesamiento de senales Master's thesis Facultad de Ingenieria, Univ. de Buenos Aires
[13] Kors J A, Van Herpen G, Sittig A C and Van Bemmel J H 1990 *European Heart Journal* **11** 1083–1092
[14] Altman D 1991 *Practical Statistics for Medical Research* (26 Boundary Row, London: Chapman Hall)
[15] Hart G 1994 *Cardiovascular Research* **28** 933–946
[16] Cooklin M, Wallis W R J, Sheridan D J and Fry C H 1997 *Circulation Research* **80** 765–771
[17] McIntosh M, Cobbe S, Kane K and Rankin A 1998 *Journal of Molecular and Cellular Cardiology* **30** 43 – 53
[18] Romhilt D and Estes E J 1968 *Am Heart J* **75** 752–58.
[19] Dilaveris P, Gialafos E, Poloniecki J, Hnatkova K, Richter D, Andrikopoulos G, Lazaki E, Gialafos J and Malik M 2000 *Clinical Cardiology* **23** 600–606